APPLICATIONS OF
MODELLING AND SIMULATION
http://arqiipubl.com/ams eISSN 2600-8084 VOL 4, 2020, 246-257

Conceptual Design of a Novel Biomimetic Underwater Robot

George G. Volanis[1*], Georgios E. Stavroulakis[1] and Konstantinos-Alketas Oungrinis[2]

[1]Computational Mechanics and Optimization Lab, School of Production Engineering and Management, Technical University of Crete, 73100 Chania, Greece
[2]Transformable Intelligent Environments Lab, School of Architectural Engineering, Technical University of Crete, 73100 Chania, Greece

[*]Corresponding author: gevolanis@gmail.com

Submitted 13 May 2020, Revised 16 June 2020, Accepted 21 June 2020.

Abstract: By defining the limits and the design specification, that an underwater robotic vehicle should fulfill in order to be characterized as biomimetic, a shell structure with a modular locomotion mechanism is proposed, using THUNDER piezoelectric, for a novel biomimetic underwater robot. Smart materials and especially piezoelectric actuators are an excellent alternative as a propulsion mechanism for our underwater swimming fish-like robot (SRFL swimming robot with fish-like locomotion), due to their unique characteristics. This paper presents the design characteristics, the restrictions in dimensions and weight of the underwater robot and the ability of it, for maneuverability. Furthermore, the articulated locomotion mechanism of the caudal fin is designed and analyzed, while the distribution of the pressure forces on the shell, as well as in the articulated mechanism of the tail fin is also determined. Finally, the articulated mechanism is represented in MATLAB/SIMSCAPE in order to simulate the locomotion of the tail fin, giving us the average speed and acceleration.

Keywords: Biomimetic robot; Fish-like shell; Piezoelectric actuator; Underwater propulsion.

1. INTRODUCTION

In this paper, an effort is made in order to contribute to the ongoing research of biomimetic robotics, which is still on the very early stage of development, even though there is access to a variety of biological data, combined with the development of low cost robotic vehicle and computer power supply systems, which are providing the necessary autonomy [1-7] using new propulsion methods such as smart materials. The conceptual design of a novel underwater robot, demands the specification of the limitations and parameters that a biomimetic robot should fulfill, regarding the preliminary design, as well as the locomotion of the caudal fin, in order to be specified as biomimetic. Through carefully studying of the corresponded bibliography, is concluded that there are three basic standards that must be fulfilled: Fish-like swimming, small scale (miniaturization), Wide tail-beat frequency and amplitude range. These standards are thoroughly examined in the next section. The term smart materials describe a group of materials that react in a controlled way when external stimulus are applied to them and as a result, they mimic biological systems and their adaptable capabilities. This reaction influences either the capabilities of the material (mechanical, electrical) or its molecular structure, or its functionality. Some of those external stimulus which react with these materials are pressure, humidity, temperature, pH, electric and magnetic fields.

Smart materials are a unique category of materials, capable of transforming other sources of energy into mechanical energy and vice versa [8-15]. The field of research regarding smart materials is interdisciplinary, as it regards a series of scientific fields, such as materials science, robotics, electrical engineering and mechanical engineering. Although their behavior has not yet been completely understood, four main categories of smart materials can be distinguished. They are:

- Materials that can change color
- Materials that can emit light
- Materials that can change temperature
- Materials that can change mechanical properties

In this study, materials that change their mechanical properties are selected, in order to create motion, and specifically applied in the field of forward actuation. Furthermore, such materials can be distinguished in six more subcategories: conductive polymers, dielectric elastomers, piezoelectric materials, polymer gel, electroactive polymers and shape memory alloys. Further, less common categories exist, such us Magneto-Rheological fluid (MRFs) and Electro-Rheological fluid (ERFs). In recent years, piezoelectric materials have been considered a promising technology for the development of non-

conventional actuators. Piezoelectric-based actuators are well suited for autonomous vehicles, operating both in land and water [16-23]. Also, they can present a high displacement ratio with high response rates and are suitable for a large range of operating frequency where the large power density can be achieved through the right mechanical design [24, 25]. They also have the ability to produce large displacements, even in small scale due to their high-pressure density and therefore they can be functional even in the mini scale [26]. Moreover, piezoelectric actuators are capable of replacing DC/AC motors, for robotics applications [27-29] where small size, and noiseless operation is required, reducing drastically power and maintenance requirements.

2. MATERIALS AND METHOD

2.1 Design characteristics of biomimetic robots

The preliminary design of an SRFL (Swimming Robots with Fish-Like Locomotion) demands a carefully determination of the three basic design specifications: Fish-Like swimming, Small scale (miniaturization), Wide tail-beat frequency and amplitude range. Even though there are other criteria, regarding the specification of the design, such as the weight and the cost, in the context of this work it will not be considered. According to Tuncdemir [25], mimicking the locomotion of the fish is not optimum for under water propulsion, but it is the most efficient compared with conventional propulsion methods. At this point should be emphasized, that it has not yet been established what type of fish swimming is optimal for achieving biomimetic propulsion. Among the other types of swimming, ostraciform [20, 30-32] is the simplest of them all, due to the high degree of freedom. In fact, the more limbs are moving, so many more joints will move respectively, which is translated to a higher degree of freedom. The presence of one joint adds one additional degree of freedom. As a result, by increasing the number of joints and subsequently the degrees of freedom, better maneuverability can be achieved. Nevertheless, as the number of joints is increased, the operational capability of the SRFL is minimized, as it would lead to a more complicated structure. Based on this, a model is designed comprised of a rigid body and one joint that controls the locomotion of the flexible caudal fin. This type of locomotion, mimics the ostraciform swimming style. The simplicity of this type of fish-like locomotion is necessary due to the fact that it minimizes the need for complicated hydro dynamical equations [33-38], making it the optimum choice for that particular swimming style. Moreover, it is not necessary to have a control mechanism for the flexible surfaces [25, 39, 40]. The SRFL proposed here is in the miniature scale [41, 42] category, in order to achieve the optimum maneuverability, abrupt acceleration and noiseless operation.

In order to mimic the locomotion of the caudal fin, first the oscillation frequency and the optimum oscillation width of the fin has been defined. Webb and Junzhi Yu [33, 43] suggests a model in order to define the push force (Body/Caudal Fin), for a given velocity. According to the work, the force from the fish to the water is correlated with the frequency and the width, of the oscillation, of the tailbeat (stroke of the caudal fin). Thus increasing frequency or the oscillation width of the tailbeat, an increase of the power that the fish produces is achieved. As result is concluded that, in the agile robotic devices, the velocity varies linearly at a rate proportionally of the power. At this stage, it must be mentioned that the heaving motion, as well as the angle of the stroke of the caudal fin are important parameters for the achievement of the desire biomimetic motion. Furthermore, the velocity of the swimming is one of the most important parameters [34, 44-46], the control of which is based on the width of oscillation, but basically is mostly depended from the rate of change of the oscillation frequency of the caudal fin. Regarding swimming velocity and the control of the direction of the SRFL, the change of the frequency of oscillation is more preferable than the change of the width [25]. This approach is the optimum, given that the frequency is a controllable parameter, compared to the value of the displacement generated at the end of the caudal fin. Finally, another decisive factor in order to achieve biomimetic locomotion is the range of operation frequency of the actuators, which determines the ability of the robot for swimming. According to Triantafyllou *et al.* [35], in order to achieve the optimum locomotion, the range of the Strouhal (St) number is defined by the boundaries:

$$0.25 \leq (St = f\frac{d}{U}) \leq 0.35 \tag{1}$$

where f is the locomotion frequency, d is the width of the wave that is created from the caudal fin (correlated with the locomotion width) and U is velocity of the robot in still waters.

The need for maneuverability is a characteristic of biomimetic locomotion, and there are two basic parameters that affect this ability. They can be quantified by means of the dimensionless numbers Froude and Maneuverability. Maneuverability is defined as the minimum rate, with which the robot is maneuvering, for a defined acceleration. On the other hand, dimensionless number Froude is interpreted as a gauge of the ability for maneuvering. The dimensionless number Froude can be obtained as

$$F_r = V/(\sqrt{(gL)}) \tag{2}$$

Subsequently,

$$F_r^4/Re = (V^4U)/(L^3g^2) \tag{3}$$

where the Reynolds number, $R_e = VL/U$, and V is the velocity, L is the kinematic viscosity and the gravity, $g = 9.81$ m/s^2.

This combined parameter can be used to rescale the coefficient of normal acceleration [34]. The fact that biomimetic robots have a huge difference in the way they accelerate, compared to fish, renders this combined parameter necessary, in order to have a successful simulation of the locomotion of the fish. Based on this, F_r is transformed to

$$F_r = V/(\sqrt{(gL)}) = (\sqrt{(L/g)})V/L = (1/2\pi)T/(L/V) \quad (4)$$

Moving forward, F_r is the function of the period, T as the time that is needed, so the body can travel a distance equal to its length. F_r has a larger value for longer and thinner fins and smaller value for shorter and thicker fins. As a result, light fins are better for having neutral buoyancy, while heavier and shorter fins force the robot to tumble minimizing the maneuverability. Finally, following the design parameters as well as the dimensional analogies of a fish robot [45], the following equations are used:

$$L_1 = 2L_2,\ 3L_1 = 10L_3,\ L_1 = 3H_1 \quad (5)$$

where L_1 is the length of the main body (rigid part), H_1 is the approximately length of the caudal fin, L_2 is the height of the main body and L_3 is the thickness of the robot. Based on these parameters, a mini robot-fish with a total body length less than 10 cm, occupies volume equal to 60 cm^3, approximately. The reduced volume minimizes the total weight and as a result minimizes the components of the robot.

2.2 Evaluation of THUNDER Actuators as Underwater Propulsors

The THUNDER (THin-layer composite Unimorphs Ferroelectric DrivEr) actuator [47-51] is a new generation of piezo ceramic actuators, capable of producing a significant amount of displacement, when electrical voltage is applied. A typical THUNDER actuator consists of two metallic materials, one slice of piezo ceramic and the adhesive film. The standard configuration is on the top one layer of metal, next goes the adhesive material, a slice of piezo ceramic, once again a film of adhesive material and at the end a metallic layer for support. The materials are united under high pressure and temperature (3000ºC) and then, they are left to cool down in a room temperature, provided that the adhesive film has solidified first. Because of the pre-stress energy that comes from the different thermal capabilities of the bonded materials when they cool down, the actuator acquires high durability and flexibility. As a result, voltages over 800 V can be applied and can withstand high displacement forces. THUNDER actuators are capable of providing displacements up to 0.5 cm [48, 52]. This capability is ideal for an underwater propulsion mechanism, even though the electromechanical efficiency and the consumption of electricity has not been registered in wet conditions, especially for underwater devices. What is known though, is that the peak of the flow rate is approximately equal to 1500 cm^3/s and also, THUNDER actuators, can create thrust greater than 4.5 N. Unfortunately, the pressure forces that are applied to the actuator are not taken into consideration, and so the real thrust has not yet been calculated. The average electrical energy that is consumed by two THUNDER actuators, inside a protective shell operating at 14 Hz is approximately 8 W, which is far less than the one consumed by other autonomous underwater vehicles.

The current electro motors have an estimated efficiency of 60% in converting electricity into thrust. The efficiency of the THUNDER actuators as propulsion mechanism is yet unknown, mainly because of the nature of piezoelectric materials that can operate also as capacitors. It is possible for THUNDER actuator to be used in a way, with the help of an inductor that the current power consumption is eliminated (parallel connection) or in order to increase enough the voltage output (serial connection). Because the electric charge is non-active, a small amount of energy is consumed during operation. The fact that the displacement response and the electric current are non-linear, lead us to the conclusion that THUNDER actuators can create thrust with low power consumption. Finally, it can operate at great depths, as it eliminates the need for sealed covers, propellers and bearings.

The THUNDER actuators used in this paper consists of a 9.5 cm × 2.54 cm × 0.254 mm steel sheet, on which is adhered a piezoceramic (PZT-5A) of 10 mil (0.254 mm) thickness. The adhesive material used is LaRc-SI of 0.6 mil (0.015239 mm) thickness. All the materials are united in high temperature ovens. Moreover, an aluminum sheet of 1 mil (0.0254 mm) thickness adhesives to the piezoceramic (PZT-5A) is used, using the same adhesive material (LaRc-SI), so that it functions as an electrode [53].

3. ARTICULATED DRIVE MECHANISM OF THE FLEXIBLE CAUDAL FIN

The research centers which focus in developing piezoelectric actuators for forward motion on water, have partially succeed in creating biomimetic locomotion for underwater environments. So, one of the purposes of this section is to present the structure and the geometry of an underwater SRFL. Furthermore, the structure of the propulsion mechanism of the SRFL, which causes the flexible caudal fin to oscillate and is positioned on the stern, is analyzed. Regarding the composition of the mechanism, the first step is to choose the desired locomotion of the caudal fin. The caudal fin is submitted to a small width oscillation (according to the length of the fin) so that it mimics the biological propulsion [53-55]. The designed articulated mechanism uses cylindrical joints, making it as the simplest way of providing one output for two inputs (Figure 1). This mechanism is similar to the dyad [40], which consists of two rigid connections fastened together, while leaving one end of each connection free. The other connection points are considered as input points and are connected to the actuator. Finally, the fin, which is made from a styrene with dimensions of 3.81 cm × 4.1275 cm × 0.254 mm, is fastened to one of the links so that the rotation point of the fin is located at the output of the articulated mechanism.

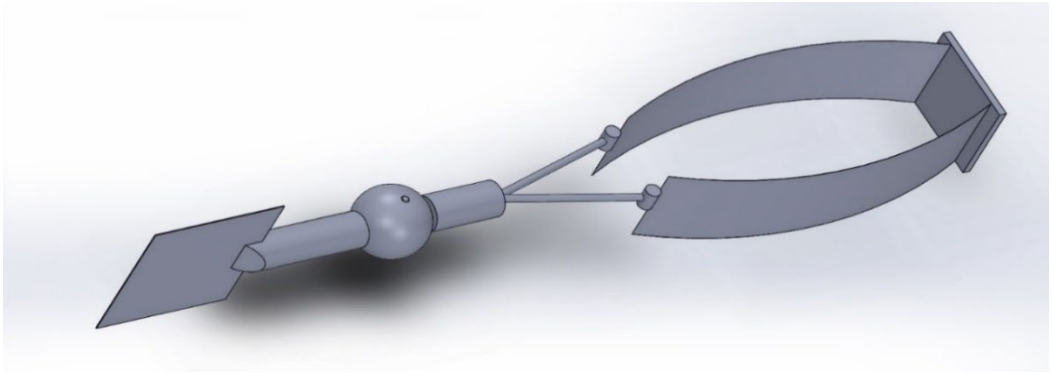

Figure 1. Representation of the articulated mechanism connected with the THUNDER actuators

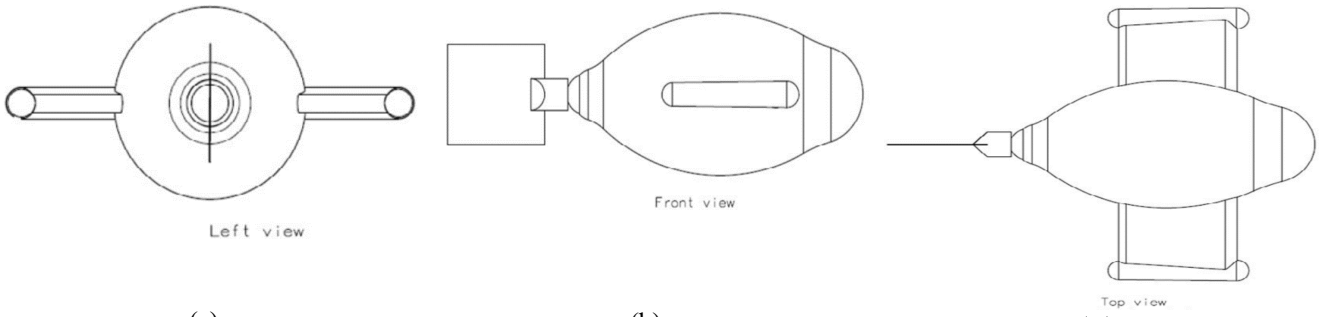

(a) (b) (c)

Figure 2. The underwater vehicle's shell. (a) Left view, (b) Front view, (c) Top view

4. MORFOLOGY OF THE UNDERWATER ROBOT'S SHELL

Following the design parameters as well as the dimensional analogies of a fish robot [45], the body length (rigid part), the height and the total width of the SRFL are 12.3825 cm, 6.19125 cm and 3.71475 cm, respectively. Meaning that, the total length is 16.51 cm and the volume is approximately 284.78 cm^3, which is by far less than the maximum permissible volume at 1000 cm^3. Figure 2 shows the final form of the SRFL. Due to the hydrodynamic restrains [56, 57], the geometry of the shell is oval. Also, this geometry allows for unobscured mounting of the drive mechanism and the digital control system, while leaving some space for extra load for various sensors. Note that the blades are positioned in a way to help maintain the robot's stability, while at the same time their shape does not adversely affect the hydrodynamics of the system.

Moving one step further in the composition of the SRFL, the blade fins are designed so that they are not fastened to the shell so that when an appropriate control system is fitted, they can be tilted upwards by 45°. The purpose of this position shift is not to act as an auxiliary mechanism to the existing one, but to exploit the hydrodynamic effects and push the robot to the surface of the sea. Note that the positions that the flaps can reason for this shift are two. The first position has a slope of 0° and the second is with the flaps sloping to 45°. By applying this mechanism, will allow the robot to move on the vertical axis as well, in order to avoid possible obstacles at the bottom of the sea. In addition, with this mechanism the coordination of the movement of the entire flock to the surface is ensured, and thus allow their collection under controlled environment.

5. DISTRIBUTION OF FORCES EXERTED ON THE SRFL DUE TO PRESSURE

The prevailing conditions of the deep ocean require a very careful design of the underwater SRFL, so that within reason, a satisfactory robotic operation is achieved. One of the main problems being dealt with, is the very high pressure forces that the SRFL shell receives due to its depth. One suggestion that could solve this painlessly is that the shell is not sealed, in order to allow the water to pass through it, so that the pressure is normalized throughout the entire robot and the pressure forces do not overwhelm the shell structure. It should be emphasized that this proposal does not adversely affect the hydrodynamics of the system. The main disadvantage is the fact that it is not possible to predict the effects of the water flowing inside the shell on the two THUNDER actuators. As mentioned in the previous section, the specifications of the THUNDER piezoelectric actuators are still under investigation, so any additional strain on the actuators cannot be calculated. For these reasons, the SRFL shell is considered sealed.

The material of the shell is a key factor in determining the strength of the robot's shell when it is subjected to a constant high pressure. In order to achieve the desired strength, an industrial steel is used, with density equal to 7860 kg/m^3, Poisson number of 0.266 and yield strength of 25×10^8 N/m^2. These properties are necessary to find the maximum pressure that the shell can accept without causing fracture. For that purpose, the finite element solver is used within the CATIA software, in order to calculate the external stress and displacement of the shell. At this point, it should be noted that the maximum value of the Von Mises strain, must be less than the value of the yield strength of the steel, so as not to cause break. Based on these limitations, the maximum pressure that the shell can accept without breaking is at 310.2641 bar, at a depth of approximately 3070.608 m.

Figure 3(a) shows the Von Mises stress table for the pressure at 310.2641 bar along with the three-dimensional representation of the stress fields received by the shell. The maximum Von Mises stress value is obtained as 2.44×10^8 N/m^2, which is less than the yield strength of the steel. The Von Mises diagram shows that the region with the highest stresses is in the center of the shell, resulting in the highest displacement at exactly this point. On the other hand, Figure 3(b) presents details of the displacement sizes, with the largest displacement of the shell being 0.036 mm. Figure 3(c) shows the areas where the estimated error is located during the simulation. Note that the error margin in the simulation values is close to zero.

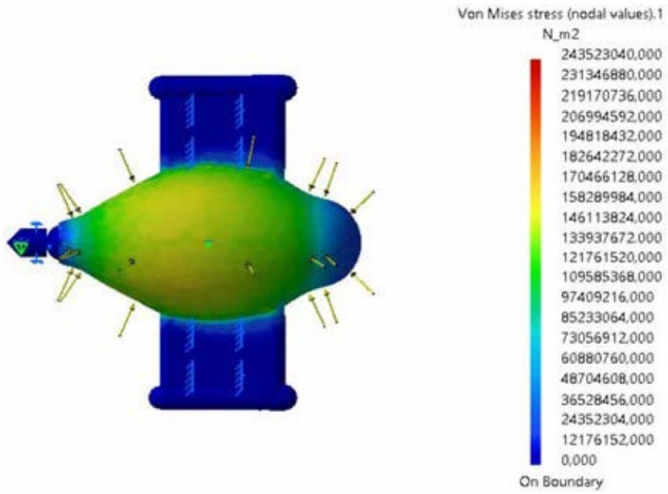

(a)

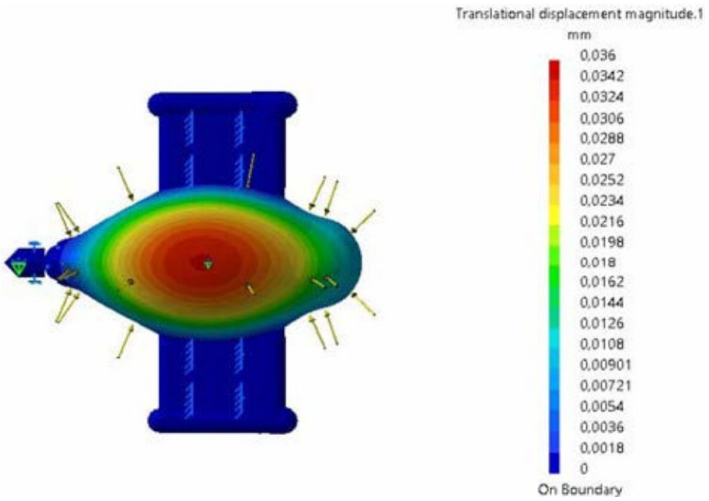

(b)

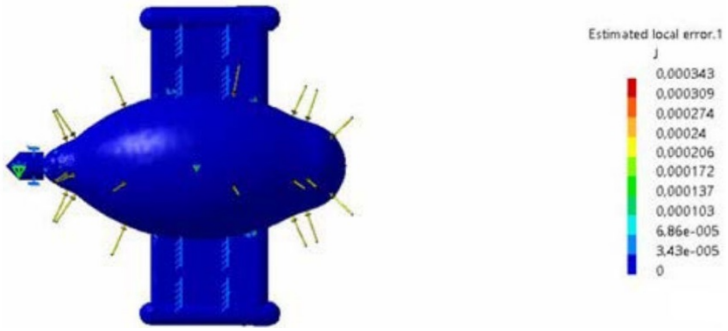

(c)

Figure 3. Results with finite element solver: (a) Stress distribution, (b) Displacement magnitude, (c) Estimated local error

6. LOCOMOTION SIMULATION

The first stage of simulation is the representation of the modular mechanism, which moves the flexible fin, in the MATLAB SIMSCAPE programming environment. In order to gain a better understanding of how the flexible caudal fin oscillates through the modular mechanism, the conditions of the biomimetic motion using the MATLAB/SIMULINK program are simulated. In addition, through simulation, the initial speed and acceleration of the submarine vehicle is estimated. On the other hand, the simulation conditions do not include the frictional forces displayed on the joint, while the damping factor is considered negligible. Also, from the specialized literature in robotics, the integrated digital control system was adopted in [39, 40], which have been already experimentally determined. According to their research, the operational frequency is settled at 160 Hz, while a signal of +300 V induces a starboard turn and the -300 V steers the vessel port.

Figure 4 shows individual parts of the articulated mechanism in MATLAB/SIMULINK program. The connection of the separate pieces creates the articulated mechanism that moves the caudal fin. Figure 5 shows in full the articulated mechanism as shown in the MATLAB programming environment. In order to achieve the best possible representation of the biomimetic motion of the caudal fin, movement is allowed only in the spherical part, which simulates the articulated joint. In addition, only one degree of freedom is selected, due to the fact that only on the *Z*-axis movement is wanted, in ordered for the rotational motion to take place around a single fixed axis. This movable joint translates to MATLAB as revolute joint. The rotational motion of this joint, and therefore the rotational motion of the entire mechanical arrangement, comes from the application of the appropriate activation signal. The displacement of THUNDER piezoelectric actuators moves the articulated mechanism of the caudal fin. In order to achieve forward motion of the vehicle and the optimal biomimetic motion of the caudal fin, these actuators must be driven by a sinusoidal vibration signal at their tuning frequency, at 160 Hz. For this reason, the revolute joint uses a sinusoidal-shaped signal with oscillation width of 25. At this point, it is important to note that the choice of this sinusoidal signal simulates the displacement produced by THUNDER actuators, which causes the oscillation of the caudal fin. In this way, optimal simulation of the conditions under which the fin oscillates is achieved and thus resulting in a simulation environment as close as possible to the real one.

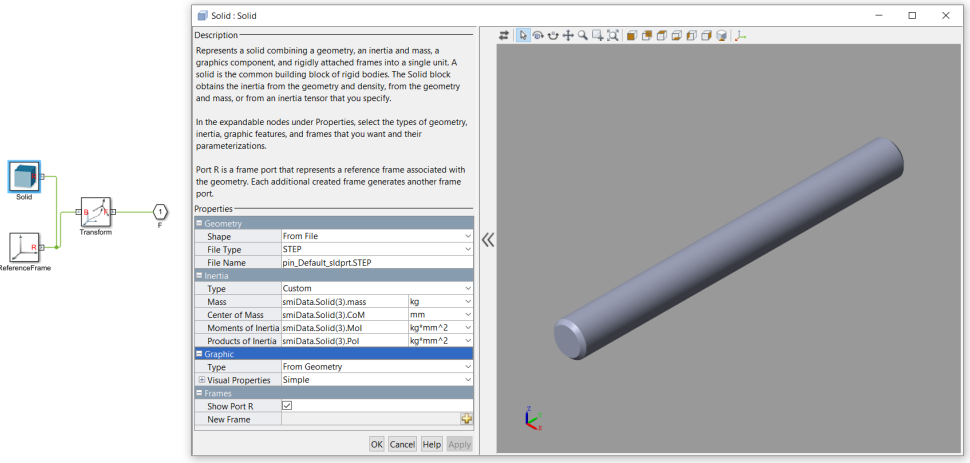

(a)

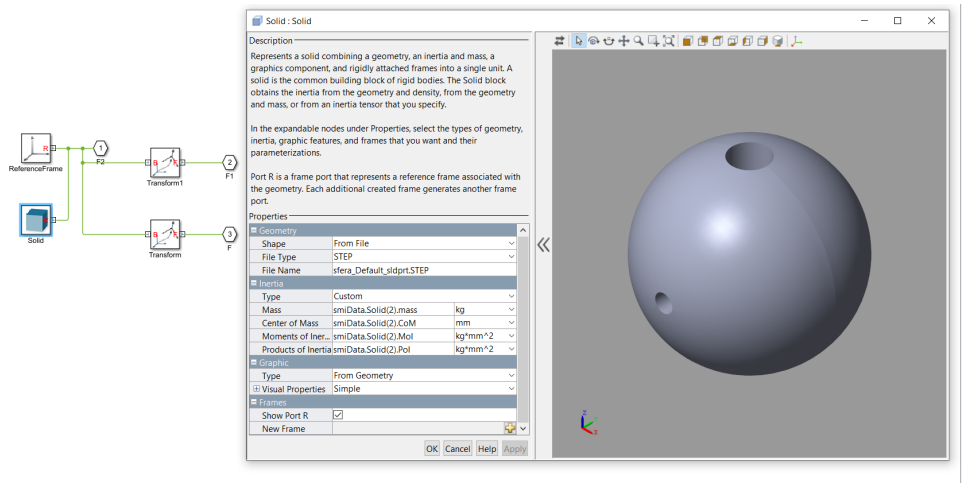

(b)

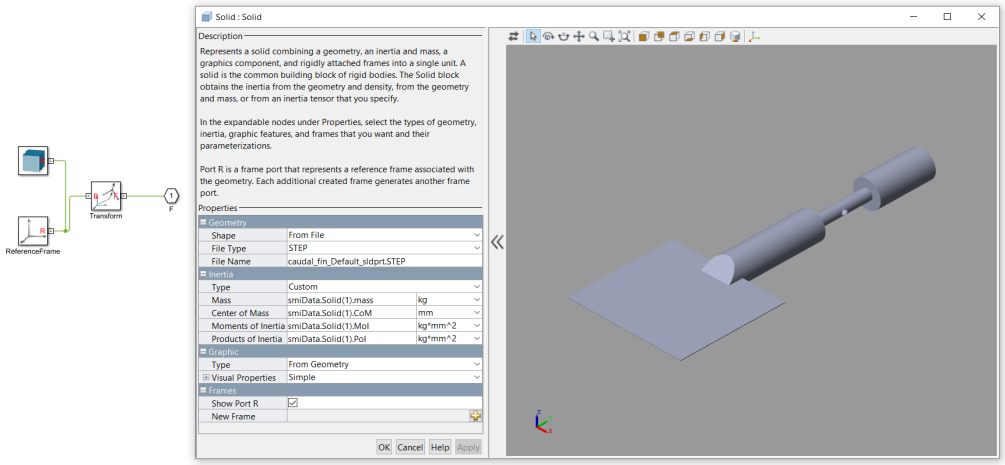

(c)

Figure 4. Individual parts of the articulated mechanism in MATLAB/SIMULINK program. (a) Rigid component which fixes the articulated mechanism on the shell stern (b) Spherical component of the articulated mechanism with one degree of freedom (c) Rigid component holding the flexible caudal fin on one end and on the other THUNDER actuators are connected.

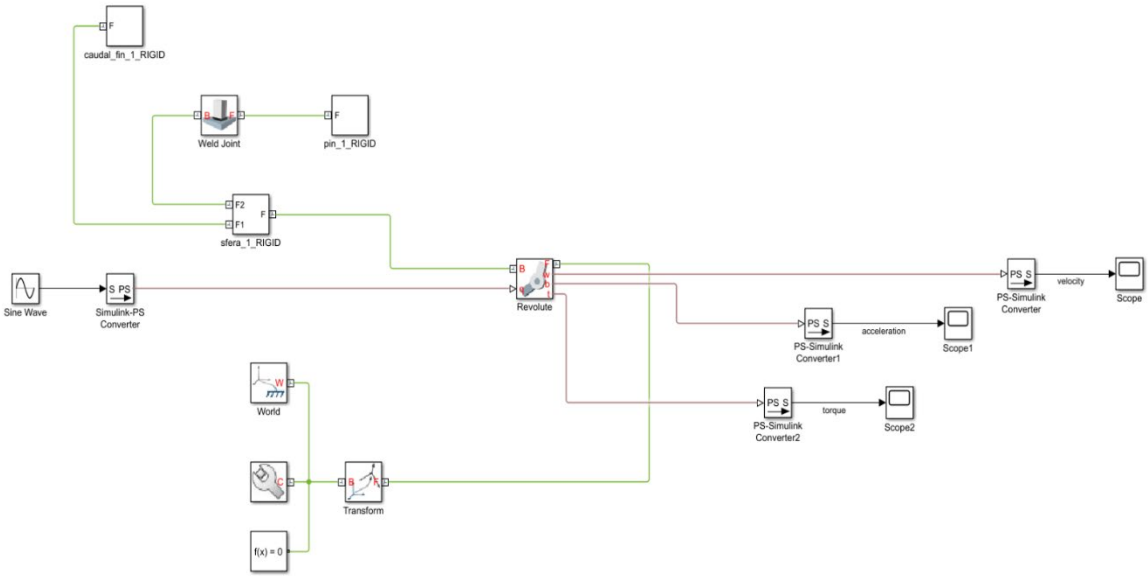

Figure 5. Assembly of the articulated mechanism and the THUNDER actuators represented on SIMSCAPE environment

Through the simulation, the angular velocity and acceleration in which the modular mechanism oscillates is successfully predicted and therefore able to accurately estimate the speed and acceleration of the SRFL submarine vehicle. Figure 6(a) shows the variation of the angular velocity with extreme values $\omega = \pm 68.01$ rad/s or $v = \pm 49$ cm/s, where the plus and minus corresponds to the direction of the vectors of velocity and acceleration. On the other hand, Figure 6(b) shows the variation of the angular acceleration, with the maximum value at time $t = 0.001$ s is $\alpha = 2.543 \times 10^4$ rad/s^2 and then decreases to $\alpha = \pm 1.087 \times 10^4$ rad/s^2 or $\alpha = \pm 780.1$ m/s^2. Going one step further, at the time $t = 0.001$ s, at the moment when the simulation starts, the maximum acceleration is $\alpha = 2.543 \times 10^4$ rad/s^2. Using $a = \alpha \times r$, where r is the distance from the center of the sphere to the end of the urethral fin, and a is the angular acceleration, a linear angular acceleration, α can be obtained as 1825.1 m/s^2.

Using the Newton's law with the mass, $m = 0.014$ kg, the maximum exerted force, F can be calculated as 25.5 N. Finally, the maximum torque produced by the modular mechanism is calculated by

$$\tau = F \times c \tag{7}$$

where c is the distance from the center of the sphere to the end of the caudal fin. With the exerted force, the maximum torque is obtained as 1.83 Nm. In the simulation conditions the frictional forces appearing on the joint are not included, while the damping factor (an indistinguishable parameter used to describe the rate with which the oscillation system declines after the disturbance) is considered negligible.

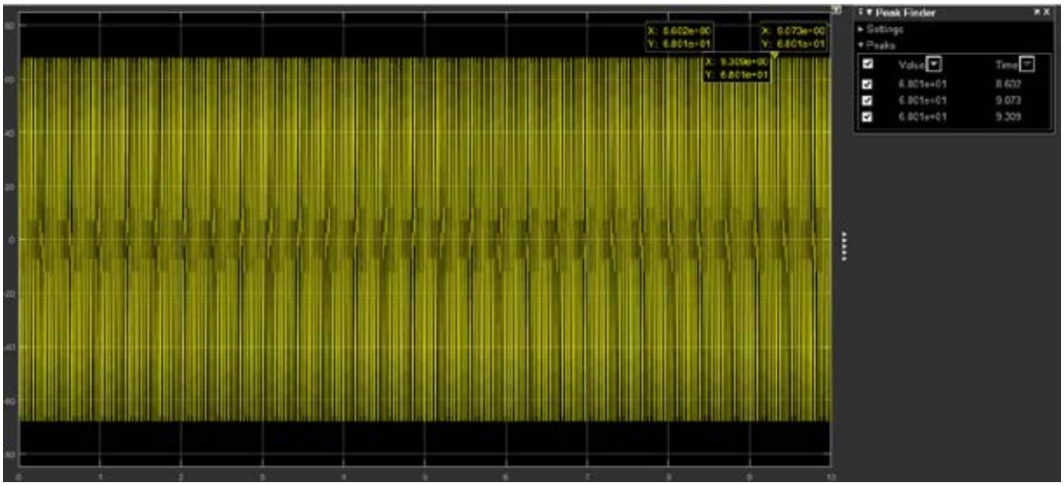

(a)

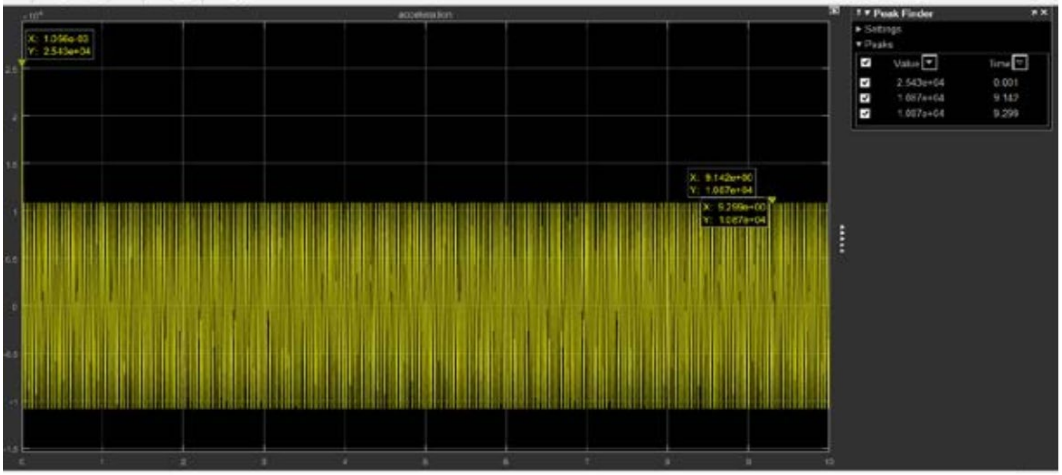

(b)

Figure 6. Variation of the response. (a) Angular velocity; (b) Angular acceleration

7. FATIGUE ANALYSIS OF THE ARTICULATED MECHANICAL ARRANGEMENT OF THE CAUDAL FIN

The biomimetic motion of the caudal fin is achieved by oscillating the articulated mechanical device, which is actuated by a sinusoidal signal with an oscillation frequency of 160 Hz. This phenomenon is particularly important because the high oscillation frequency results in an increase in the rate of fatigue of the modular mechanism, due to the inertial forces exerted on the flexible blade as well as on the mechanical device that moves it. In order to achieve an acceptable level of endurance on the modular mechanism against these stresses, and at the same time having a smoother operation for a longer period of time, high-carbon industrial steel, Carbon Steel 1023 is selected in this work. The characteristic of the steel is shown in Table 1.

Table 1. Characteristic of the high carbon steel

Property	Value	Unit
Elastic modulus	$2.049999984 \times 10^{11}$	N/m^2
Poisson's ratio	0.29	
Sheer modulus	$7.999999987 \times 10^{10}$	N/m^2
Mass density	7858	kg/m^3
Tensile strength	425000003.2	N/m^2
Yield strength	282685049	N/m^2
Thermal expansion coeffiecient	1.2×10^{-5}	/K

The maximum value of the Von Mises voltage must be less than the value of the yield strength of the steel at 282,685,049 N/m^2 so as not to cause breakage. Figure 7 show the Von Mises stress table with the inertial forces straining the modular mechanism is 25.5 N. Note that the areas with the greatest stress are located at the points where the pieces are connected to each other, with the highest value being at 202,355,872 N/m^2 at the connection point with the flexible caudal fin. However, the inertial forces displayed on the modular mechanism are less than the yield strength of the steel. The areas with the highest stresses (equivalent strain) are determined, as shown in Figure 8(a), with the maximum deformation being 4.345×10^{-4}. Finally,

Figure 8(b) shows the fatigue of the articulated mechanism due to the inertial forces for a period equal to 1 billion cycles of rotation. It is observed that the inertial forces received by the mechanism cause a local breakage at the point of connection with the caudal fin after 452,785,906 million cycles of rotation, as shown in Figure 9. One could argue that the local rupture at the junction of the flexible wing with the modular mechanism, after 452,785,906 million cycles, causes permanent disability in the biomimetic propulsion of the vehicle. However, it is important to note that such problems can be easily addressed by using rapid standardization methods for fixed parts.

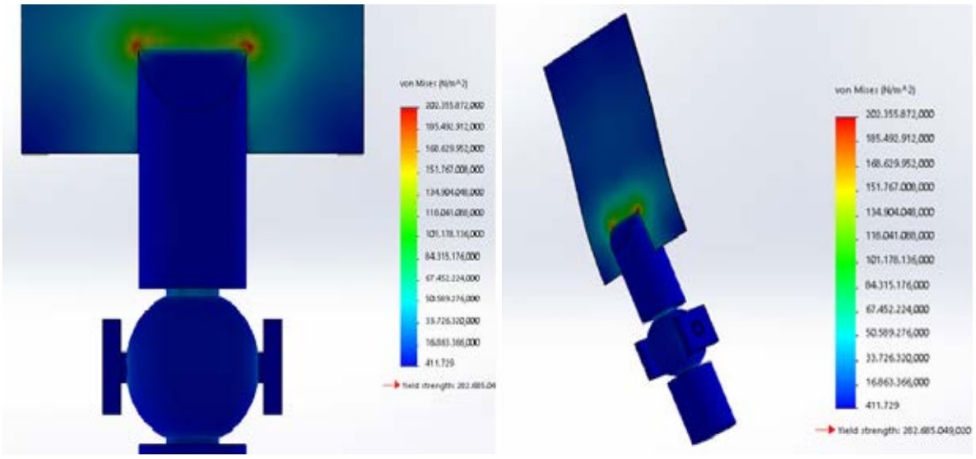

Figure 7. Stress distribution on the caudal fin

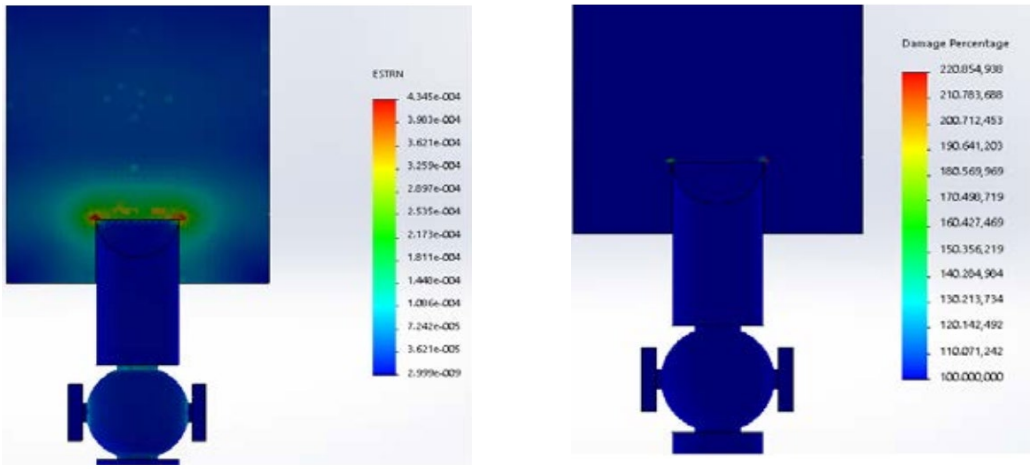

(a) (b)

Figure 8. (a) Distribution of strain and deformation; (b) Fatigue damage equal to one billion cycles of rotation

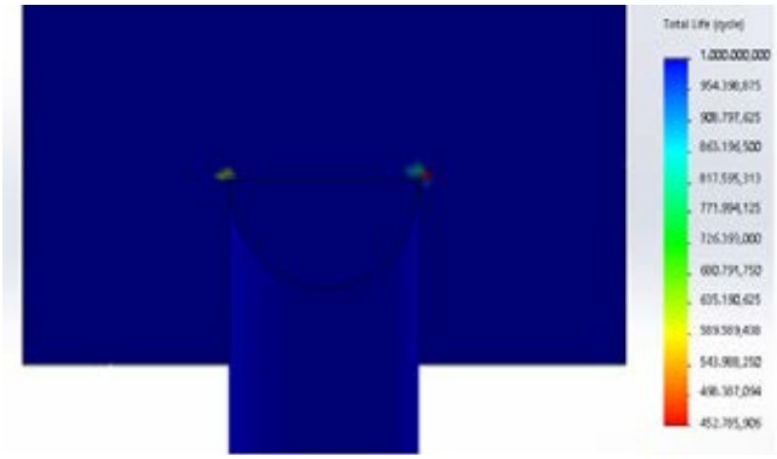

Figure 9. The points where the first breakage appears after 452,785,906 million cycles of rotation

8. CONCLUSION

In the present work, the shell and the articulated mechanism that oscillates the caudal flexible fin of a prototype underwater biomimetic vehicle, was designed. The vehicle uses as a propulsion mechanism, the displacement generated by the THUNDER piezoelectric actuators, when a controlled electric voltage is applied to them at an operational frequency of 160 Hz. Using this data, a locomotion simulation is conducted, using MATLAB/SIMSCAPE and successfully concluded that the angular velocity of the SRFL is $v = 49$ cm/s and the average acceleration is $a = 780.1$ m/s^2. Also, the stress analysis proved that the shell designed can endure a maximum pressure without breaking at 310.2641 bar, at a depth of approximately 3,070.608 m. On the other hand, the fatigue analysis of the caudal fin showed that, the inertial forces $F = 25.5$ N received by the mechanism cause a local breakage at the point of connection with the caudal fin after 452,785,906 million cycles of rotation. It should be emphasized that the characteristics of the underwater vehicle are mainly obtained from corresponded bibliography, lacking in experimental verification. As a result, it is unable to determine the complex hydro dynamical phenomena that take place during the locomotion of the caudal fin [33-38, 43, 44, 58], forming a wave pump mechanism that creates a flow around the body's turning points and thus making it impossible to determine the actual turning speed and acceleration. Studying and understanding these phenomena will be helpful to demonstrate a most accurate simulation of the movement of the modular mechanism. Possible improvements in the simulation could be made by integrating the two piezoelectric devices into the modular drive mechanism in the MATLAB/SIMSCAPE environment. Also, the optimization of the shell and the material from which it will be made, depending on the conditions in which it will operate (depth, temperature, bottom morphology, intensity of sea currents), as well as of the function that will be called to perform (e.g. oceanography, finding shipwrecks, mapping of submarine archeological sites), is the subject of a careful study.

ACKNOWLEDGEMENT

The paper is based on the Diploma Thesis of S.C.S. done under the supervision of Professor Dr. Georgios E. Stavroulakis for the Integrated Master Degree at the Technical University of Crete.

REFERENCES

[1] J. E. Clark, J. G. Cham, S. A. Bailey, E. M. Froehlich, P. K. Nahata, R. J. Full and M. R. Cutkosky, Biomimetic design and fabrication of a hexapedal running robot, *Proceedings of the IEEE International Conference on Robotics and Automation*, Seoul, South Korea, 2001, 1-6.

[2] Maki K. Habib, Keigo Watanabe and Kiyotaka Izumi, Biomimetics robots, from bio-inspiration to implementation, *33rd Annual Conference of the IEEE Industrial Electronics Society (IECON)*, Taipei, Taiwan, 2007, 1-5.

[3] J. Ayers, C. Wilbur and C. Olcott, Lamprey Robots, *Proceedings of the International Symposium on Aqua Biomechanisms*, Japan, 2000, 1-6.

[4] D. W. Thompson, *On Growth and Form*. New York, USA: The McMillan Company, 1945.

[5] N. Plamondon and M. Nahon, Adaptive controller for a biomimetic underwater vehicle, *Journal of Unmanned Vehicle Systems*, 1(1), 2013, 1-13.

[6] M. Li, S. Guo, J. Guo, H. Hirata and H. Ishihara, Development of a biomimetic underwater microrobot for a father–son robot system, *Microsystem Technologies*, 23, 2017, 849-861.

[7] S. Guo, L. Shi, N. Xiao and K. Asaka, A biomimetic underwater microrobot with multifunctional locomotion, *Robotics and Autonomous Systems*, 60(12), 1472-1483.

[8] M. Shahinpoor and K. J. Kim, Ionic polymer–metal composites: IV. Industrial and medical applications, *Smart Materials and Structures*, 14, 2005, 197-214.

[9] D. W. Robinson, J. E. Pratt, D. J. Paluska and G. A. Pratt, Series elastic actuator development for a biomimetic walking robot, *Proceedings of the 1999 IEEE/ASME International Conference on Advanced Intelligent Mechatronics*, Atlanta, USA, 1999, 1-7.

[10] M. Shahinpoor, Y. Bar-Cohenz, J. O. Simpsonx and J. Smith, Ionic polymer–metal composites (IPMCs) as biomimetic sensors, actuators and artificial muscles-a review, *Smart Materials and Structures*, 7(6), 1998, R15-R30.

[11] S.-W. Yeom, I.-K. Oh, A biomimetic jellyfish robot based on ionic polymer metal composite actuators, *Smart Materials and Structures*, 18(8), 2009, 085002.

[12] M. Sitti, D. Campolo, J. Yan and R. S. Fearing, Development of PZT and PZN-PT based unimorph actuators for micromechanical flapping mechanisms, *Proceedings of the 2001 IEEE International Conference on Robotics & Automation*, Seoul, Korea, 2001, 3839-3846.

[13] H. Shin, S. Jo and A. G. Mikos, Biomimetic materials for tissue engineering, *Biomaterials*, 24(24), 2003, 4353-4364.

[14] J. Najem, S. A. Sarles, B. Akle and D. J. Leo, Biomimetic jellyfish-inspired underwater vehicle actuated by ionic polymer metal composite actuators, *Smart Materials and Structures*, 21(9), 2012, 094026.

[15] Q. Shen, T. Wang, K. J. Kim, A biomimetic underwater vehicle actuated by waves with ionic polymer-metal composite soft sensors, *Bioinspiration & Biomimetics*, 10(5), 2015, 055007.

[16] M. Shahinpoor and K. J. Kim, Ionic polymer–metal composites: III. Modeling and simulation as biomimetic sensors, actuators, transducers, and artificial muscles, *Smart Materials and Structures*, 13(6), 2004, 1362-1388.

[17] A. A. Yumaryanto, J. An and S. Lee, A cockroach-inspired hexapod robot actuated by LIPCA, *IEEE Conference on Robotics, Automation and Mechatronics*, Bangkok, Thailand, 2006, 1-6.

[18] N. Lobontiu, M. Goldfarb and E. Garcia, A piezoelectric-driven inchworm locomotion device, *Mechanism and Machine Theory*, 36(4), 2001, 425-443.

[19] S. Heo, T. Wiguna, H. C. Park and N. S. Goo, Effect of an artificial caudal fin on the performance of a biomimetic fish robot propelled by piezoelectric actuators, *Journal of Bionic Engineering*, 4(3), 2007, 151-158.
[20] W.-S. Chu, K.-T. Lee, S.-H. Song, M.-W. Han, J.-Y. Lee, H.-S. Kim, M.-S. Kim, Y.-J. Park, K.-J. Cho and S.-H. Ahn, Review of biomimetic underwater robots using smart actuators, *International Journal of Precision Engineering and Manufacturing*, 13, 2012, 1281-1292.
[21] N. Kamamichi, M. Yamakita, K. Asaka and Z.-W. Luo, A snake-like swimming robot using IPMC actuator/sensor, *Proceedings of the 2006 IEEE International Conference on Robotics and Automation*, Florida, 2006, 1812-1817.
[22] R. S. Fearing, K. H. Chiang, M. H. Dickinson, D. L. Pick, M. Sitti and J. Yan, Wing transmission for a micromechanical flying insect, *Proceedings of the 2000 IEEE International Conference on Robotics & Automation*, San Francisco, 2000, 1509-1516.
[23] S. Guo, T. Fukuda and K. Asaka, A new type of fish-like underwater microrobot, *IEEE/ASME Transactions on Mechatronics*, 8(1), 2003, 136-141.
[24] B. F. Smith, *Development and characterization of a mechanically prestressed piezoelectric composite*, Thesis, Virginia Commonwealth University, USA, 2008.
[25] S. Tunçdemir, *Design of mini swimming robot using piezoelectric actuator*, Thesis, School of Natural and Applied Sciences, Middle East Technical University, Turkey, 2004.
[26] L. Wang, Y. Hou, K. Zhao, H. Shen, Z. Wang, C. Zhao and X. Lu, A novel piezoelectric inertial rotary motor for actuating micro underwater vehicles, *Sensor and Actuator A: Physical*, 295, 2019, 428-438.
[27] T. Salumäe, R. Raag, J. Rebane, A. Ernits, G. Toming, M. Ratas and M. Kruusmaa, Design principle of a biomimetic underwater robot U-CAT, *2014 OCEAN*, St. John's, NL, Canada, 2014, 1-5.
[28] S. B. Behbahani and X. Tan, Bio-inspired flexible joints with passive feathering for robotic fish pectoral fins, *Bioinspiration & Biomimetics*, 11(3), 2016, 036009.
[29] C. Zhou and K. H. Low, Design and locomotion control of a biomimetic underwater vehicle with fin propulsion, *IEEE/ASME Transactions on Mechatronics*, 17(1), 2012, 25-33.
[30] Y. Terada and I. Yamamoto, An animatronic system including lifelike robotic fish, *Proceedings of the IEEE*, 92(11), 2004, 1814-1820.
[31] M. Sfakiotakis, D. M. Lane, J. Bruce and C. Davies, Review of fish swimming modes for aquatic locomotion, *IEEE Journal of Oceanic Engineering*, 24(2), 1999, 237-252.
[32] P. Szymak, Mathematical model of underwater vehicle with undulating propulsion, *Third International Conference on Mathematics and Computers in Sciences and in Industry*, Chania, Greece, 2016, 269-274.
[33] P. W. Webb, Is the high cost of body caudal fin undulatory swimming due to the increased friction drag or inertial recoil?, *Journal of Experimental Biology*, 162, 1992, 157-166.
[34] M. S. Triantafyllou and G. S. Triantafyllou, An efficient swimming machine, *Scientific American*, 272(3), 1995, 64-70.
[35] G. S. Triantafyllou, M. S. Triantafyllou and M. A. Grosenbaugh, Thrust development in oscillating foild with application to fish propulsion, *Journal of Fluids and Structures*, 7(2), 1993, 205-224.
[36] Z. Guan, N. Gu, W. Gao and S. Nahavandi, 3D hydrodynamic analysis of a biomimetic robot fish, *11th International Conference on Control, Automation, Robotics and Vision*, Singapore, 2010, 793-798.
[37] Y.-J. Park, U. Jeong, J. Lee, S.-R. Kwon, H.-Y. Kim and K.-J. Cho, Kinematic condition for maximizing the thrust of a robotic fish using a compliant caudal fin, *IEEE Transactions on Robotics*, 28(6), 2012, 1216-1227.
[38] P. Szymak and M. Przybylski, Thrust measurement of biomimetic underwater vehicle with undulating propulsion, *Scientific Journal of Polish Naval Academy*, 213(2), 2018, 69-82.
[39] M. G. Borgen, *Design of a miniature, piezoelectrically actuated swimming vehicle*, Thesis, The Ohio State University, USA, 2001.
[40] M. G. Borgen, G. N. Washington and G. L. Kinzel, Design and evolution of a piezoelectrically actuated miniature swimming vehicle, *IEEE/ASME Transactions on Mechatronics*, 8(1), 2003, 66-76.
[41] W. Trimmer and R. Jebens, Actuators for micro robots, *IEEE Conference on Robotics and Automation*, Scottsdale, USA, 1989, 1547-1552.
[42] P. Dario, R. Valleggi, M. C. Carrozza, M. C. Montesi and M. Cocco, Microactuators for microrobots: a critical survey, *Journal of Micromechanics and Microengineering*, 2(3), 1992, 141-157.
[43] J. Yu, M. Tan, S. Wang and E. Chen, Development of a biomimetic robotic fish and its control algorithm, *IEEE Transactions on Systems, Man, and Cybernetics, Part B (Cybernetics),* 34(4), 2004, 1798-1810.
[44] M. Sfakiotakis, D. M. Lane and B. C. Davies, An experimental undulating-fin device using the parallel bellows actuators, *Proceedings of the 2001 IEEE International Conference on Robotics and Automation*, South Korea, 2001, 2356-2362.
[45] D. Tzeranis, E. Papadopoulos and G. Triantafyllou, On the design of an autonomous robot fish, *Proceedings of 11th IEEE Mediterranean Conference on Control and Automation (MED03)*, Rhodes, 2003, 1-6.
[46] Q.-P. Wei, S. Wang, X. Dong, L.-J. Shang and M. Tan, Design and kinetic analysis of a biomimetic underwater vehicle with two undulating long-fins, *Acta Automatica Sinica*, 39(8), 2013, 1330-1338.
[47] K. M. Mossi, R. P. Bishop, R. C. Smith and H. T. Banks, Evaluation criteria for THUNDER^{TM} actuators, *SPIE Conference on Mathematics and Control in Smart Structures*, Newport Beach, California, 1999, 738-743.
[48] S. Balakrishnan and C. Niezrecki, Investigation of THUNDER^{TM} actuators as underwater propulsors, *Journal of Intelligent Material Systems and Structures*, 13(4), 2002, 193-207.
[49] J. L. Pinkerton and R. W. Moses, A feasibility study to control airfoil shape using THUNDER, *NASA Technical Memorandum 4747*, 1997, 1-26.

[50] K. M. Mossi and R. P. Bishop, Characterization of different types of high performance THUNDER™ actuators, *SPIE Conference on Mathematics and Control in Smart Structures*, Newport Beach, California, 1999, 43-52.
[51] Z. Ounaies, K. Mossi, R. Smith and J. Bernd, Low-field and high-field characterization of THUNDER actuators, *Proceedings of SPIE Smart Structures and Materials 2001: Active Materials: Behavior and Mechanics*, 4333, 2001, 399-407.
[52] C. Niezrecki and S. Balakrishnan, Power characterization of THUNDER™ actuators as underwater propulsors, *Proceedings of SPIE: Smart Structures and Materials 2001: Smart Structures and Integrated Systems*, 4327, 2001, 88-98.
[53] H. P. Urbach, On optimum propulsion by means of periodic motion of rigid profile II. Optimization of the period and numerical results, *Studies in Applied Mathematics*, 82, 1990, 181-215.
[54] H. P. Urbach, Existence of optimum propulsion by means of periodic motion of rigid profile, *Studies in Applied Mathematics*, 81, 1989, 93-116.
[55] D. Costa, G. Palmieri, M.-C. Palpacelli, M. Callegari and D. Scaradozzi, Design of a bio-inspired underwater vehicle, *12th IEEE/ASME International Conference on Mechatronic and Embedded Systems and Applications (MESA)*, Auckland, New Zealand, 2016, 1-6.
[56] P. R. Bandyopadhyay, Maneuvering hydrodynamics of fish and small underwater vehicles, *Integrative and Comparative Biology*, 42(1), 2002, 102-117.
[57] D. S. Barrett, M. S. Triantafyllou, D. K. P. Yue, M. A. Grosenbaugh and M. J. Wolfgang, Drag reduction in fish-like locomotion, *Journal of Fluid Mechanics*, 392, 1999, 183-212.
[58] S. J. Park et al., Phototactic guidance of a tissue-engineered soft-robotic ray, *Science*, 353(6295), 2016, 158-162.